ISSN 0869-5938, Stratigraphy and Geological Correlation, 2022, Vol. 30, No. 2, pp. 75–88. © Pleiades Publishing, Ltd., 2022.
Russian Text © The Author(s), 2022, published in Stratigrafiya, Geologicheskaya Korrelyatsiya, 2022, Vol. 30, No. 3, pp. 25–40.

Age and Geodynamic Setting of the Lower Jurassic Sandstones in the Onon Fragment of the Aga Terrane, Mongol–Okhotsk Fold Belt

Yu. N. Smirnova[a], * and Yu. V. Smirnov[a]

[a] *Institute of Geology and Nature Management, Far Eastern Branch, Russian Academy of Sciences, Blagoveshchensk, 675000 Russia*

**e-mail: smirnova@ascnet.ru*

Received April 13, 2021; revised November 15, 2021; accepted December 7, 2021

Abstract—This paper presents the results of geochemical studies of sandstones of the Aga–Borshchovochnyi complex in the Onon fragment of the Aga Terrane (Tutkhaltui Valley) within the Mongol–Okhotsk Fold Belt, as well as the results of U–Th–Pb (LA-ICP-MS) geochronological and Lu–Hf isotope geochemical studies of detrital zircons from these rocks. It was established that the youngest population of detrital zircons in the studied sandstones has an age of 196 ± 8 Ma. This indicates the Early Jurassic age of the sediments that were previously dated as Middle Paleozoic. The geochemical features of sandstones suggest that they were deposited in the active continental margin or island arc setting at the final stage of the closure of the Mongol–Okhotsk Paleocean.

Keywords: Mongol–Okhotsk Fold Belt, Aga Terrane, Early Jurassic, sedimentary rocks, sources, detrital zircons, U–Th–Pb and Lu–Hf studies

DOI: 10.1134/S0869593822030054

INTRODUCTION

The Mongol–Okhotsk Fold Belt extends as a narrow strip from Central Mongolia to the Sea of Okhotsk and represents a mosaic of exotic terranes (Badarch et al., 2002; *Geodinamika*..., 2006; Nokleberg et al., 2005; Parfenov et al., 2001; Wang et al., 2015; etc.). According to the current understanding (Metelkin et al., 2010; Parfenov et al., 2003; Tomurtogoo et al., 2005; Zhao et al., 1990; Zonenshain et al., 1990; Zorin, 1999; etc.), it was formed in the place of the paleocean of the same name as a result of convergence of the Siberian Craton and the Amur Microcontinent. Most geodynamic models of its formation, based on geological and paleontological data, suggest the gradual closure of the ocean and the rejuvenation of its constituent complexes in the northeastern direction (Parfenov et al., 2003; Tomurtogoo et al., 2005; Zonenshain et al., 1990; etc.). There is also a model of the nonsimultaneous (segmental) closure of the Mongol–Okhotsk Paleocean (Arzhannikova et al., 2022; Didenko et al., 2010; etc.).

Two types of terranes have been recognized within the accretionary prism of the Mongol–Okhotsk Fold Belt (Parfenov et al., 2001). The terranes of the first (A) type are composed predominantly of turbidites, volcanic–siliceous rocks, and limestones, whereas the terranes of the second (B) type contain fragments of ophiolites in addition to greenschists, siliceous–argillaceous, argillaceous, and siliceous rocks, and limestones (Parfenov et al., 2001). A large body of geological, geochemical, geochronological, and isotope geochemical data on the Paleozoic and Mesozoic sedimentary sequences has been accumulated thus far for the western (Arzhannikova et al., 2020, 2022; Bussien et al., 2011; Demonterova et al., 2017; Hara et al., 2013; Kelty et al., 2008; Popeko et al., 2020; Yang et al., 2015; etc.) and eastern (Sorokin et al., 2015; Sorokin et al., 2020; Zaika and Sorokin, 2020a, 2020b; etc.) segments of the Mongol–Okhotsk Fold Belt. However, the existing geodynamic models of its formation are still disputable in many aspects. It should be noted that particularly interesting is the reconstruction of the Mesozoic evolution of the Mongol–Okhotsk Belt, which included the closure of the paleocean.

The western segment of the Mongol–Okhotsk Fold Belt comprises the Aga Terrane, which consists of several fragments (subterranes) (Badarch et al., 2002; Parfenov et al., 2001; Ruzhentsev and Nekrasov, 2009; etc.). In Eastern Transbaikalia, it is represented by the Onon (Onon–Kulinda) fragment. The stratified rocks of the Onon fragment include the Upper Proterozoic (?) (Amantov, 1975) or Middle Paleozoic (Rutshtein et al., 2019; Shivokhin et al., 2010) siliceous, carbonate, terrigenous–carbonate, and volcanic rocks of the Aga–Borshchovochnyi complex,

unconformably overlain by the fossiliferous Upper Paleozoic sedimentary rocks of the Chiron Group with a total thickness of 3200–4200 m. The section ends with the Permian and Triassic marine sediments (Parfenov et al., 2001; Rutshtein et al., 2019; Ruzhentsev and Nekrasov, 2009; Shivokhin et al., 2010). The youngest marine sediments in the Onon fragment of the Aga Terrane are the terrigenous and volcanic rocks of the Kamenka Formation. The age of the Kamenka Formation has not been established accurately. The sandstones and siltstones of this formation were found to contain Early Triassic plant detritus (*Cladophlebis* sp., *Czekanowskia* sp.), whereas the K–Ar isotopic age of the volcanic rocks of this formation is Triassic–Early Jurassic (245–187 Ma; Shivokhin et al., 2010).

Systematic geochronological (U–Pb) studies within the Onon fragment of the Aga Terrane were carried out earlier only for igneous rocks. It was established that the ages of the gabbro and plagiogranites of the Tsugol Massif at the boundary between the Aga Terrane and the Argun Superterrane are 448 ± 9 Ma (U–Th–Pb method, SIMS) and 436 ± 4 Ma (U–Pb method, ID TIMS), respectively (Lykhin et al., 2007; Ruzhentsev and Nekrasov, 2009). Devonian gabbro (415–388 Ma, U–Th–Pb method, SIMS) (Ruzhentsev and Nekrasov, 2009) was established in the northeast of the aforementioned fragment of the Aga Terrane. At the same time, sedimentary rocks that compose the Onon fragment of the Aga Terrane are less well studied. Integrated studies of greenschists of the Aga–Borshchovochnyi dynamometamorphic complex in the Nynken River basin were carried out not long ago. It was found that the lower limiting depositional age of their protoliths, according to U–Th–Pb datings (LA-ICP-MS) of detrital zircons, corresponds to the Late Cambrian (492 ± 6 Ma; Popeko et al., 2020), which contradicts the current understanding of the age of the Aga–Borshchovochnyi complex (Amantov, 1975; Rutshtein et al., 2019; Shivokhin et al., 2010). In this connection, we performed the geochemical studies of sandstones in the Tutkhaltui Valley as well as the U–Th–Pb (LA-ICP-MS) geochronological and Lu–Hf isotopic geochemical studies of the detrital zircons extracted from them. On the latest geological maps (Rutshtein et al., 2019; Shivokhin et al., 2010), these sandstones are ascribed to the Middle Paleozoic phyllite subcomplex of the Aga–Borshchovochnyi dynamometamorphic complex.

GEOLOGICAL POSITION AND PETROGRAPHIC FEATURES OF THE SANDSTONES

According to the tectonic maps of the western part of the Mongol–Okhotsk Fold Belt (Gordienko et al., 2019; Ruzhentsev and Nekrasov, 2009; Shivokhin et al., 2010), the Onon fragment of the Aga Terrane borders on the Selenga–Stanovoi Fold Belt in the north and the Khentei–Daur Terrane in the west and has been thrust onto the rocks of the Argun Superterrane in the east.

The marginal part of the Aga Terrane is composed of the rocks of the Aga–Borshchovochnyi complex (Bogach, 2000; Rutshtein et al., 2019; Shivokhin et al., 2010), which were earlier (Tulokhonov, 1962) classified as the Kulinda and Onon formations. The Aga–Borshchovochnyi complex has been subdivided into two subcomplexes. The first, phyllite, subcomplex is composed of phyllonites and albite–quartz–sericite, albite–sericite–quartz, and carbonaceous quartz–sericite schists. The second, greenschist, subcomplex is composed of albite–epidote–chlorite, albite–chlorite–epidote–actinolite, sericite–quartz, quartz–sericite, and carbonaceous quartz–sericite schists, quartzites, and marbles. The age of the rocks of the Aga–Borshchovochnyi complex is considered as Middle Paleozoic (Shivokhin et al., 2010). At the same time, Rutshtein (2000) admitted that some fragments of the Aga–Borshchovochnyi complex had a longer (Paleozoic–Early Mesozoic) formation history.

In order to identify the main sources of detrital material and specify the lower limiting depositional age of the rocks of the Aga–Borshchovochnyi complex within the Onon fragment of the Aga Terrane, we performed an analysis of the geochemical composition of sandstones collected in the Tutkhaltui Valley, as well as U–Th–Pb (LA-ICP-MS) geochronological and Lu–Hf isotope geochemical studies of detrital zircons extracted from these rocks (Fig. 1).

Samples in our collection consist predominantly of gray and brownish gray sandstones with fine- to coarse-grained psammitic texture and massive structure. The sandstones are composed of angular and subrounded fragments of quartz and feldspar, as well as fragments of felsic volcanic rocks, sericite–quartz schists, and epidote–siliceous and epidote–siliceous–actinolite schists. Calcite is scarce. Micas occur as occasional biotite (often chloritized) and muscovite flakes. The contact and pore-filling cement is composed of illite. Accessory minerals are zircon, sphene, apatite, garnet, and magnetite. The sandstones are characterized by poorly sorted clastic material.

ANALYTICAL METHODS

The abundances of rock-forming elements and Zr in rocks were determined by the X-ray fluorescence method on a Pioneer 4S X-ray spectrometer at the Institute of Geology and Nature Management, Far Eastern Branch, Russian Academy of Sciences (Blagoveshchensk), and the abundances of trace elements (Li, Ga, Rb, Sr, Ba, La, Ce, Pr, Nd, Sm, Eu, Gd, Tb, Dy, Ho, Er, Tm, Yb, Lu, Y, Nb, Ta, Th, U, Pb, Sc, V, Cr, Co, Ni, Cu, and Zn) were determined by the ICP-MS method with an Elan 6100 DRC mass spectrometer at the Institute of Tectonics and Geophysics, Far

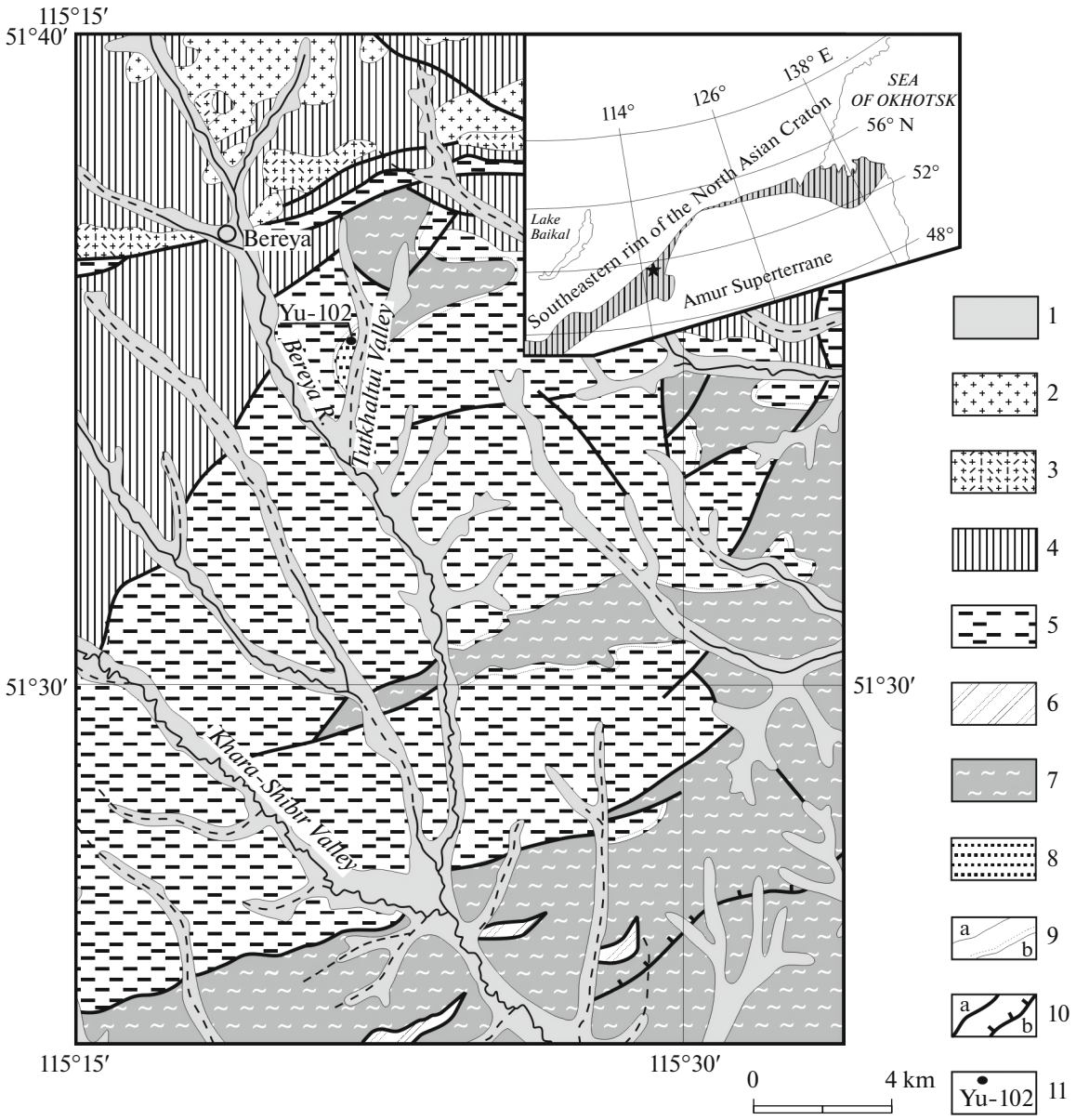

Fig. 1. Simplified geological map of the Onon fragment of the Aga Terrane. Modified after (Shivokhin et al., 2010) and (Rutshtein et al., 2019). (1) Cenozoic loose sediments; (2) Bereya plagiogranite complex, Late Triassic; (3) Kamenka andesite–dacite complex, Late Triassic; (4) Upper Triassic sedimentary rocks; (5) Upper Paleozoic sedimentary rocks of the Chiron Basin; (6) Middle–Upper Devonian sedimentary and volcano-sedimentary rocks of the Ust-Borzya Formation; (7) Middle Paleozoic rocks of the Aga–Borshchovochnyi complex; (8) surface outcrops of the studied Lower Jurassic sandstones of the Tutkhaltui Valley; (9) proven conformable (a) and unconformable (b) contacts of stratigraphic units; (10) faults (a) and thrust faults (b); (11) sampling site for U–Th–Pb geochronological and Lu–Hf isotope geochemical studies and sample number. Inset map: asterisk indicates the area under study; crosshatched area is the Mongol–Okhotsk Fold Belt.

Eastern Branch, Russian Academy of Sciences (Khabarovsk). The powdered samples were homogenized for X-ray fluorescence analysis by fusing with a flux of lithium metaborate and tetraborate in a muffle furnace at a temperature of 1050–1100°C. Analytical line intensities were corrected for the background and the effects of absorption and secondary fluorescence in the course of analysis. The uncovering of the samples in order to determine minor element abundances by the ICP-MS method was carried out by acid decomposition. Calibration of mass spectrometer sensitivity over the whole scale of masses was carried out using standard solutions containing all elements analyzed. The uncertainty of estimates of abundances of rock-forming elements and trace elements was 3–10%.

Detrital zircons were extracted at the Mineralogical Laboratory of the Institute of Geology and Nature Management with the aid of heavy liquids. The U–

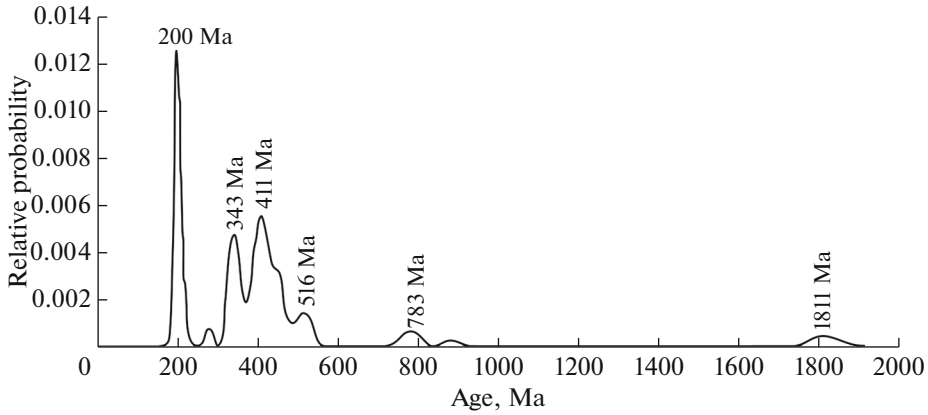

Fig. 2. Relative probability curve of the ages of detrital zircons from the sandstone collected in the Tutkhaltui Valley of the Onon fragment of the Aga Terrane (Sample Yu-102).

Th–Pb dating of individual zircon grains was carried out at the Arizona LaserChron Center of the University of Arizona, United States, with a Thermo Element 2 ICP mass spectrometer, equipped with a Photon Machines Analyte G2 laser ablation system. The crater was 20 μm in diameter with a depth of 15 μm. A detailed description of the analytical procedures is available on the laboratory website (www.laserchron.org). The concordant ages were calculated with the Isoplot v. 3.6 software (Ludwig, 2008). Only these ages were used for plotting relative age probability curves of detrital zircons.

The Lu–Hf isotope geochemical studies of zircons were also performed at the Arizona LaserChron Center of the University of Arizona using a Nu high-resolution multicollector mass spectrometer with inductively coupled plasma (MC-ICP-MS) with an Analyte G2 excimer laser. It should be noted that the Lu–Hf isotope analyses were performed in the zircon grain zones for which the U–Th–Pb dating was performed. Details of the analytical procedures are available on the laboratory website (www.laserchron.org). $\varepsilon_{Hf(t)}$ values were computed using the ^{176}Lu decay constant ($\lambda = 1.867e^{-11}$) after (Sherer et al., 2001; Söderlund et al., 2004) and the chondritic $^{176}Hf/^{177}Hf$ (0.282785) and $^{176}Lu/^{177}Hf$ (0.0336) ratios after (Bouvier et al., 2008). Crustal Hf model ages, $t_{Hf(C)}$, were calculated on the basis of the average value of the $^{176}Lu/^{177}Hf$ ratio of 0.0093 in the continental crust (Amelin and Davis, 2005; Vervoort and Patchett, 1996). The isotopic parameters of the depleted mantle were calculated using the present-day values of $^{176}Hf/^{177}Hf = 0.28325$ and $^{176}Lu/^{177}Hf = 0.0384$ (Griffin et al., 2004).

THE RESULTS OF U–Th–Pb (LA-ICP-MS) GEOCHRONOLOGICAL AND Lu-Hf ISOTOPE GEOCHEMICAL STUDIES

Concordant age estimates were obtained for 73 of the 121 detrital zircon grains extracted from the sandstone. The predominant part of zircons yielded Paleozoic (281–531 Ma) and Mesozoic (195–222 Ma) ages. Neoproterozoic (769–884 Ma) and Paleoproterozoic (1802–1849 Ma) zircons occur in smaller amounts. The main peaks on the relative probability curve correspond to 200, 343, 411, 516, 783, and 1811 Ma (Fig. 2). The youngest detrital zircon population has an age of 196 ± 8 Ma. The zircons differ in morphology and zoning pattern. The Paleozoic and Mesozoic zircons are represented predominantly by bipyramidal–prismatic crystals with a distinct oscillatory zoning (Figs. 3a–3e), which indicates the initially igneous origin of the zircons. The oldest Neo- and Paleoproterozoic zircons are represented by rounded grains (Fig. 3f)

The isotope geochemical (Lu–Hf) studies were performed on nine zircon grains characterized by concordant age values. It was established that the Paleozoic detrital zircons are characterized by slightly negative and positive $\varepsilon_{Hf(t)}$ values varying from –1.4 to +7.7 and $t_{Hf(C)}$ in the interval of 0.7–1.3 Ga, whereas the Early Jurassic zircons display near-zero $\varepsilon_{Hf(t)}$ values ranging from –1.4 to +1.2 with $t_{Hf(C)}$ in the interval of 1.0–1. 1 Ga (Fig. 4, Table 1).

GEOCHEMICAL FEATURES OF THE SANDSTONES

The chemical composition of sedimentary rocks provides information about the paleotectonic settings of sediment accumulation and the composition and a degree of chemical "maturity" of rocks in the source areas. The established chemical compositions of representative Lower Jurassic sandstone samples are given in Table 2. On the $\log(SiO_2/A_2O_3)$–$\log(Na_2O/K_2O)$ (Pettijohn et al., 1976) and $\log(SiO_2/Al_2O_3)$–$\log(Fe_2O_3/K_2O)$ (Herron, 1988) classification diagrams, they correspond predominantly to greywacke (Figs. 5a, 5b).

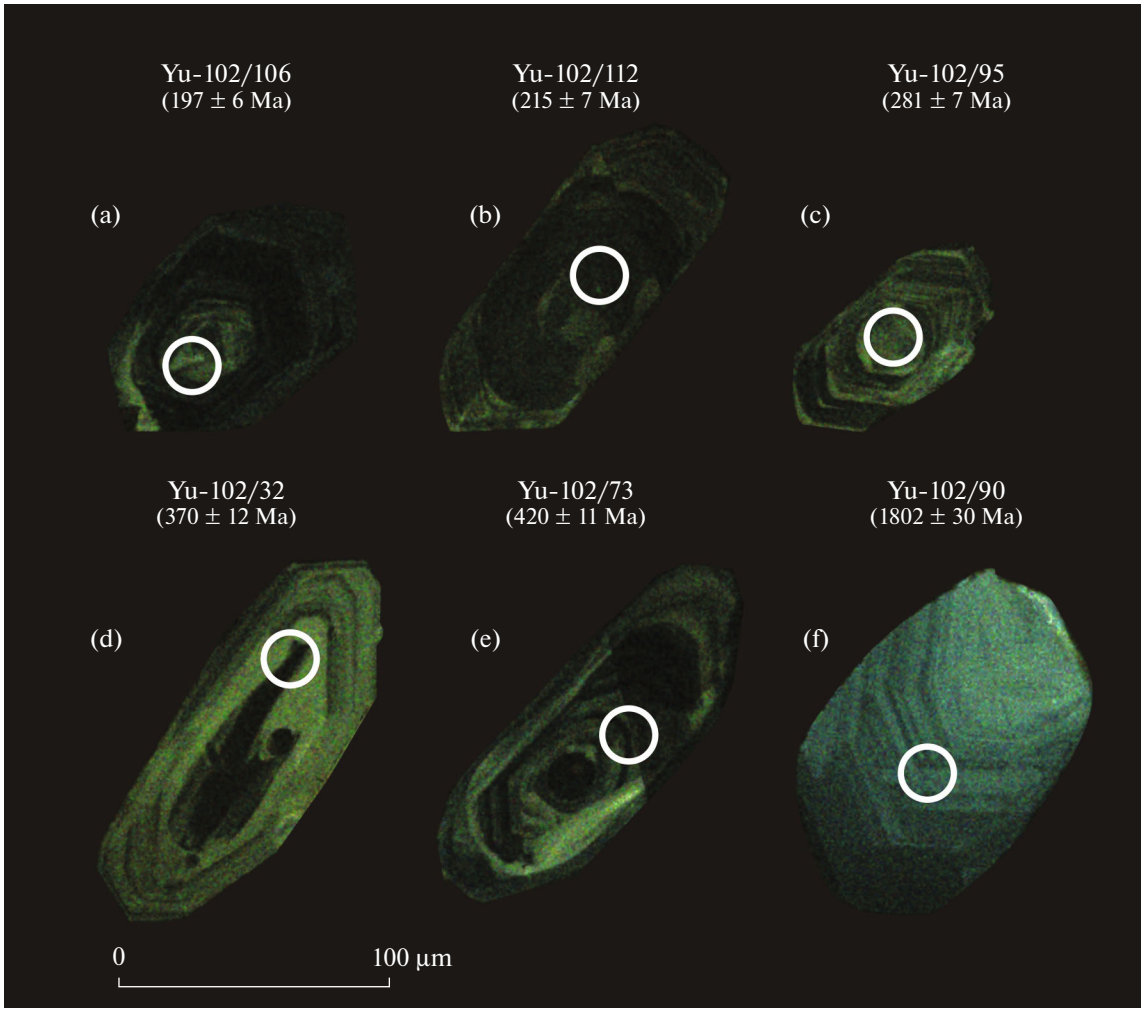

Fig. 3. Cathodoluminescence images of detrital zircon grains from a sample of Lower Jurassic sandstone collected in the Onon fragment of the Aga Terrane (Sample Yu-102).

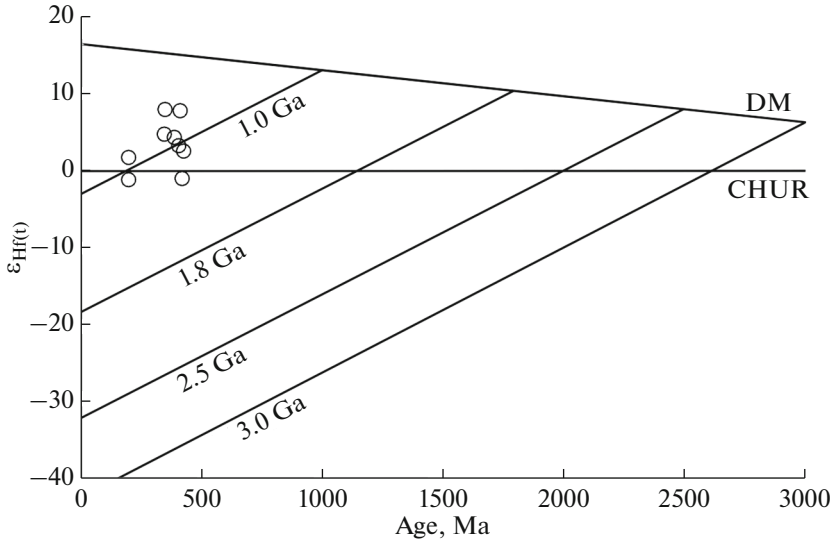

Fig. 4. Age versus $\varepsilon_{Hf(t)}$ plot for detrital zircons from the Lower Jurassic sandstone collected in the Onon fragment of the Aga Terrane (Sample Yu-102). Abbreviations: DM, depleted mantle; CHUR, chondritic uniform reservoir.

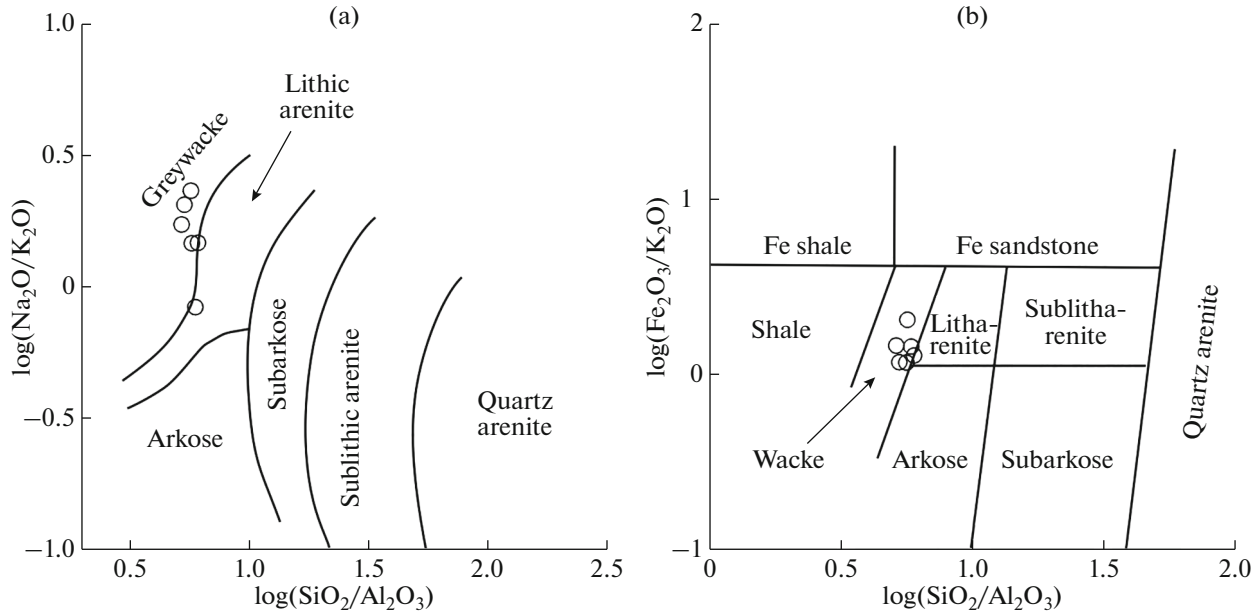

Fig. 5. Diagrams (a) $\log(SiO_2/Al_2O_3)$–$\log(Na_2O/K_2O)$ (Pettijohn et al., 1976) and (b) $\log(SiO_2/Al_2O_3)$–$\log(Fe_2O_3/K_2O)$ (Herron, 1988) for the Lower Jurassic sandstones in the Onon fragment of the Aga Terrane.

The Lower Jurassic sandstones are close to sediments originating from felsic protoliths in terms of the content of major rock-forming components represented on Na_2O–CaO–K_2O (Bhatia, 1983) and (CaO + MgO)–$SiO_2/10$–(Na_2O + K_2O) (Taylor and McLennan, 1985) plots (Figs. 6a, 6b). A similar conclusion also ensues from Th–La–Sc (Cullers, 2002), Hf–Th–Co (Wronkiewicz and Condie, 1987), La/Sc–Th/Co (Cullers, 2002), and Hf–La/Th (Floyd and Leveridge, 1987) plots (Fig. 6c–6f). In addition, the felsic composition of rocks in the source areas is also indicated by the pattern of distribution of rare-earth elements. Indeed, the total REE concentrations in the Lower Jurassic sandstones vary from 126 to 183 μg/g (Table 2). The distribution of lanthanides is moderately differentiated ($[La/Yb]_n$ values are from 7.29 to 15.55) with a pronounced negative europium anomaly (Eu/Eu* in the interval of 0.61–0.68) (Fig. 7a).

The concentrations of most trace elements in the studied sandstones are close to those in the upper continental crust with a slight deficiency in Nb, Ta, and Sr (Fig. 7b). Worthy of mentioning are the low concentrations of the "transition" trace elements (Sc, Co, V, and Ni). Similar concentrations of these elements are typical of the Phanerozoic felsic and intermediate igneous rocks (Condie, 1993).

The sandstones are characterized by moderate values of the chemical index of weathering (CIW) (Harnois, 1988) and high values of the silica titanium index (STI) (Jayawardena and Izawa, 1994) (Table 2), which

Table 1. Results of the Lu–Hf isotope geochemical studies of detrital zircons from sandstone of the Tutkhaltui Valley (Sample Yu-102)

No.	Sample index/ Grain number	Age, Ma	$(^{176}Yb + ^{176}Lu)/^{176}Hf$ (%)	$^{176}Lu/^{177}Hf$	$^{176}Hf/^{177}Hf$	± (1σ)	$\varepsilon_{Hf(t)}$	$t_{Hf(DM)}$	$t_{Hf(C)}$
1	Yu-102/17	197	52.8	0.003129	0.282695	0.000021	1.2	0.8	1.0
2	Yu-102/21	200	19.5	0.001236	0.282612	0.000017	−1.4	0.9	1.1
3	Yu-102/100	346	15.2	0.000968	0.282690	0.000016	4.5	0.8	0.9
4	Yu-102/40	348	9.2	0.000660	0.282778	0.000013	7.7	0.7	0.7
5	Yu-102/101	388	12.8	0.000806	0.282652	0.000018	4.1	0.8	1.0
6	Yu-102/15	406	8.6	0.000588	0.282609	0.000019	3.0	0.9	1.0
7	Yu-102/36	411	10.3	0.000652	0.282735	0.000015	7.6	0.7	0.8
8	Yu-102/85	421	15.1	0.000963	0.282478	0.000018	−1.4	1.1	1.3
9	Yu-102/74	425	30.9	0.002121	0.282580	0.000021	2.0	1.0	1.1

The uncertainties (1σ) of the $^{176}Hf/^{177}Hf$ estimates correspond to the last significant digits after the decimal point.

Table 2. Chemical composition of representative samples of the Lower Jurassic sandstones in the Onon fragment of the Aga Terrane

Sample/components	Yu-102	Yu-102-1	Yu-102-2	Yu-102-4	Yu-102-5	Yu-102-10
SiO_2	69.64	70.74	68.52	69.86	68.48	72.18
TiO_2	0.57	0.50	0.66	0.44	0.55	0.38
Al_2O_3	12.15	12.45	11.56	13.09	13.18	11.87
$Fe_2O_3^*$	4.73	2.76	4.85	2.88	3.78	3.25
MnO	0.06	0.05	0.10	0.06	0.05	0.04
MgO	1.29	0.87	1.41	1.03	1.24	0.98
CaO	2.37	1.91	1.96	1.63	1.97	1.63
Na_2O	3.34	5.43	2.79	4.99	4.42	3.69
K_2O	2.28	2.34	3.33	2.43	2.56	2.51
P_2O_5	0.10	0.17	0.19	0.13	0.15	0.16
LOI	2.24	1.17	2.74	1.54	1.82	1.69
Total	98.77	98.39	98.11	98.08	98.20	98.38
Li	21.65	22.25	28.80	22.05	28.77	19.85
Rb	77	65	116	67	72	75
Sr	126	231	220	240	217	192
Ba	375	598	798	661	634	558
La	23.37	32.73	39.14	38.24	37.30	29.90
Ce	53.42	69.18	80.16	76.84	77.40	60.53
Pr	5.81	7.06	8.34	7.77	7.68	6.44
Nd	23.19	26.93	32.19	29.43	29.27	22.17
Sm	4.54	4.80	5.74	5.24	5.15	3.84
Eu	1.01	0.90	1.16	1.02	1.02	0.74
Gd	4.37	3.98	5.17	4.70	4.69	3.42
Tb	0.63	0.53	0.73	0.70	0.67	0.48
Dy	3.86	2.81	4.20	4.21	4.13	2.83
Ho	0.71	0.48	0.75	0.77	0.76	0.52
Er	2.27	1.49	2.40	2.48	2.50	1.65
Tm	0.30	0.20	0.33	0.34	0.34	0.23
Yb	2.18	1.43	2.28	2.41	2.50	1.68
Lu	0.30	0.20	0.32	0.34	0.35	0.24
Y	18	12	20	20	20	13
Th	7.68	10.68	12.26	12.21	13.65	11.32
U	2.00	2.16	1.96	2.40	3.04	2.25
Zr	209	180	212	354	315	265
Hf	3.15	1.60	2.96	2.59	2.82	2.66
Nb	8	10	13	10	11	9
Ta	0.69	0.77	0.94	0.86	0.88	0.80
Zn	58	63	89	47	56	40
Co	6	4	8	4	4	3
Ni	12	5	14	6	6	5
Sc	7.0	5.2	8.2	5.8	7.9	4.2
V	43	41	65	45	58	34
Cr	65	56	45	65	51	56
Pb	13	13	21	13	15	13
Eu/Eu*	0.68	0.61	0.64	0.61	0.62	0.61
$[La/Yb]_n$	7.29	15.55	11.65	10.77	10.13	12.11
ΣREE	126	153	183	174	174	135
CIW	55	50	59	54	55	57
STI	86	87	85	87	86	88

Oxides are given in wt %; elements, in μg/g. $Fe_2O_3^*$, total iron expressed as Fe_2O_3. $CIW = (Al_2O_3/(Al_2O_3 + CaO + Na_2O)) \times 100$ (Harnois, 1988); $STI = ((SiO_2/TiO_2)/((SiO_2/TiO_2) + (Al_2O_3/TiO_2) + (SiO_2/Al_2O_3))) \times 100$ (Jayawardena and Izawa, 1994).

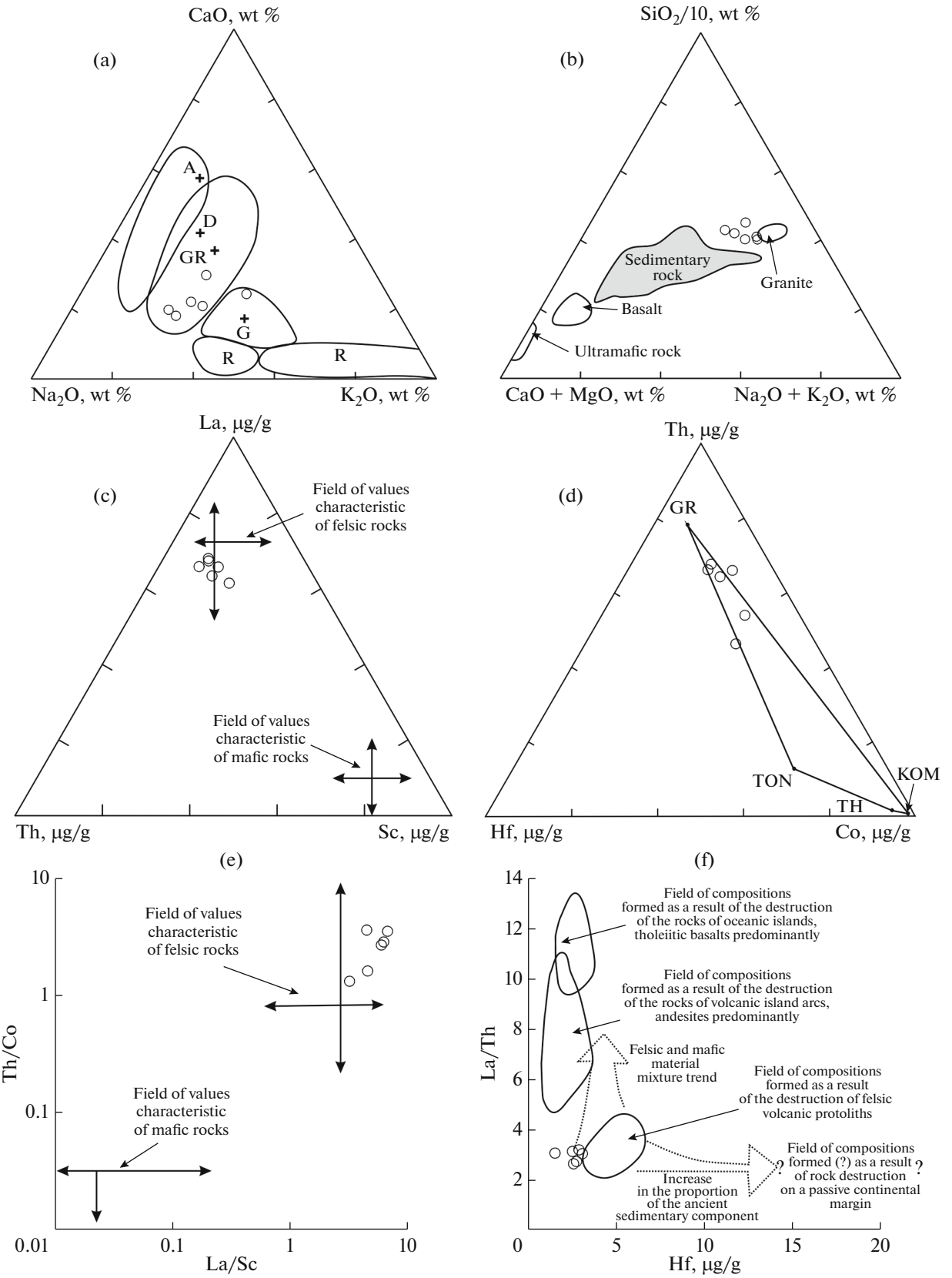

Fig. 6. Diagrams (a) Na_2O–CaO–K_2O (Bhatia, 1983), (b) (CaO + MgO)–SiO_2/10-(Na_2O + K_2O) (Taylor and McLennan, 1985), (c) Th–La–Sc (Cullers, 2002), (d) Hf–Th–Co (Wronkiewicz and Condie, 1987), (e) La/Sc–Th/Co (Cullers, 2002), and (f) Hf–La/Th (Floyd and Leveridge, 1987) for the Lower Jurassic sandstones in the Onon fragment of the Aga Terrane. Abbreviations: (a) A, andesite; D, dacite; GR, granodiorite; G, granite; R, recycled sediments; (d) GR, granite; TON, tonalite; TH, tholeiite; KOM, komatiite.

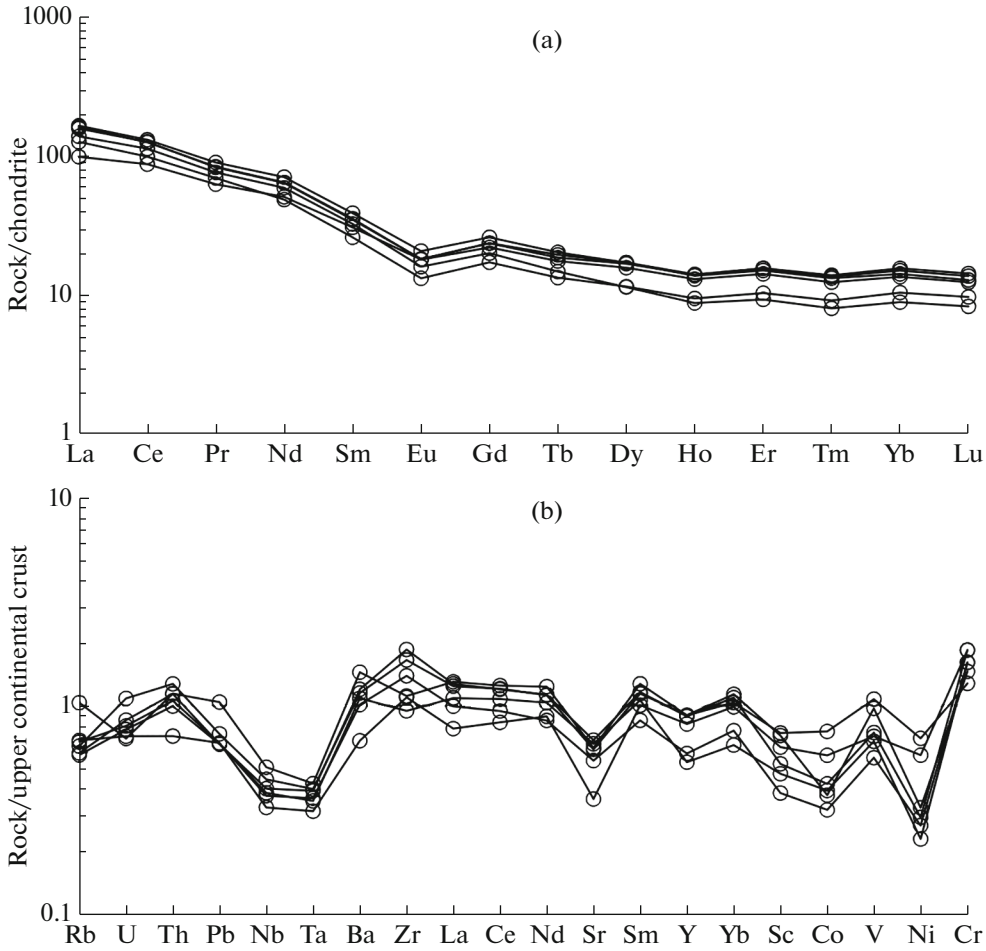

Fig. 7. Plot of distribution of rare-earth elements (a) and spider diagram (b) for the Lower Jurassic sandstones in the Onon fragment of the Aga Terrane. Chondrite compositions are after (McDonough and Sun, 1995); upper continental crust compositions are after (Taylor and McLennan, 1985).

attests to the predominantly mechanical destruction of rocks with a subordinate role of chemical weathering.

The paleotectonic setting of the Lower Jurassic sandstone accumulation process was reconstructed using the $(Fe_2O_3^* + MgO)–K_2O/Na_2O$, $(Fe_2O_3^* + MgO)–Al_2O_3/(CaO + Na_2O)$, $(Fe_2O_3^* + MgO)–Al_2O_3/SiO_2$, and $(Fe_2O_3^* + MgO)–TiO_2$ diagrams (Bhatia, 1983). Sandstone composition points on these diagrams are located in the field of sedimentary rocks accumulated in the setting of an active continental margin and continental island arc (Fig. 8). On the Th–La diagram (Bhatia and Crook, 1986) the studied sandstones tend to the field of compositions typical of sandstones in a continental island arc (Fig. 9a). A similar conclusion follows from the F1–F2 diagram (Bhatia, 1983) (Fig. 9b). On the basis of the analysis of the concentrations of major rock-forming components in sedimentary rocks, a new $DF1_{(Arc–Rift–Col)}–DF2_{(Arc–Rift–Col)}$ discrimination diagram was proposed (Verma and Armstrong-Altrin, 2013). The Lower Jurassic sandstones are characterized by high SiO_2 concentrations (68.48–72.18 wt %, Table 2); in this connection, the paleotectonic setting of their accumulation was determined using the $DF1_{(Arc–Rift–Col)m1}–DF2_{(Arc–Rift–Col)m1}$ diagram with fields for highly siliceous sedimentary rocks. Sandstone composition points based on $DF1_{(Arc–Rift–Col)m1}$ and $DF2_{(Arc–Rift–Col)m1}$ values are located along the line that separates sediments accumulated in island arc and continental rift settings (Fig. 9c).

DISCUSSION

The results of our studies were fairly unexpected. Firstly, the youngest population of detrital zircons from the sandstones collected in the Tutkhaltui Valley and previously assigned to the Aga–Borshchovochnyi complex yielded an Early Jurassic age (196 ± 8 Ma). These datings contradict the concept of the Riphean (Amantov, 1975) and Middle Paleozoic (Rutshtein et al., 2019; Shivokhin et al., 2010) age of the rocks of the Aga–Borshchovochnyi complex. Considering that

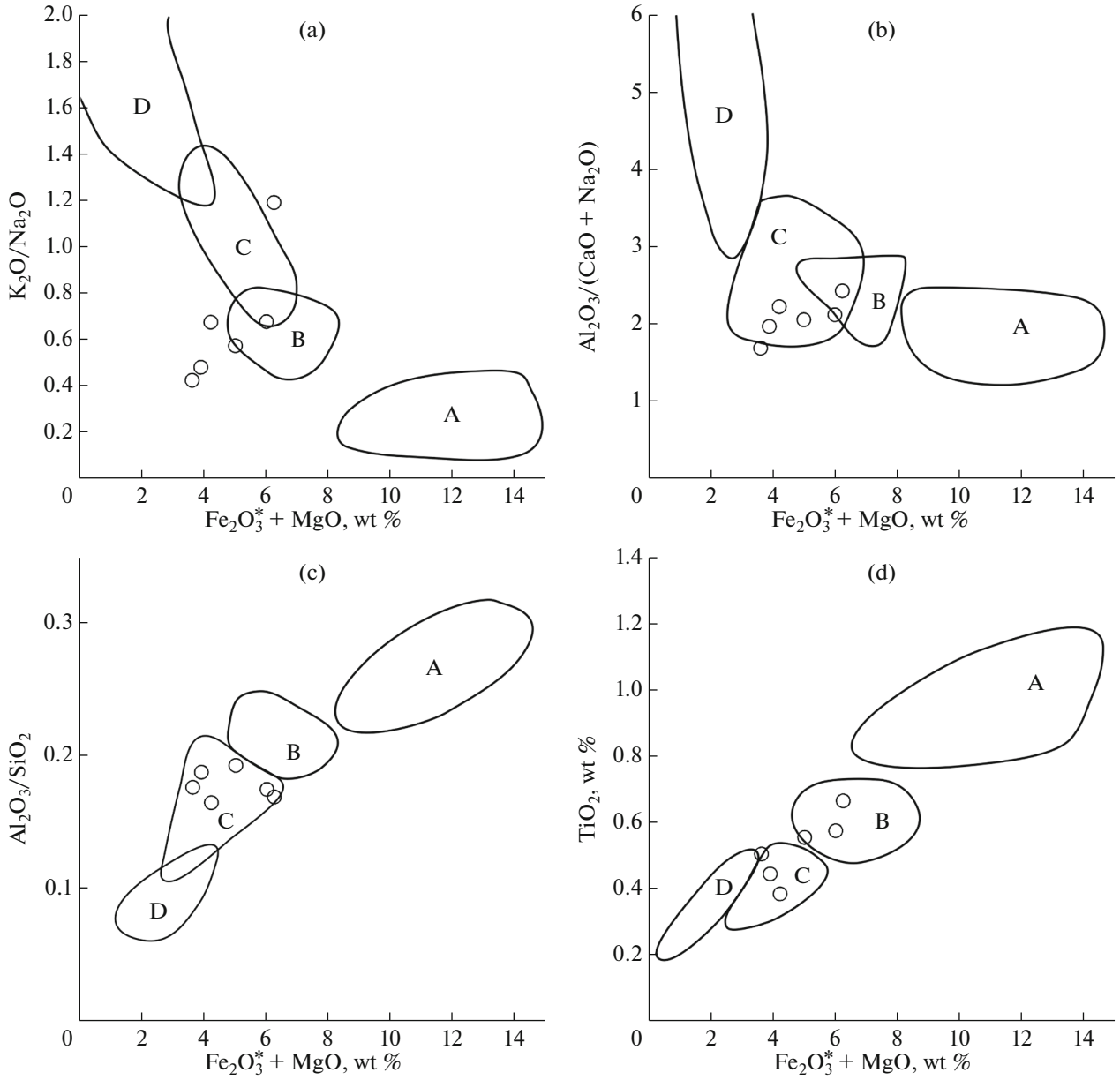

Fig. 8. Diagrams (a) ($Fe_2O_3^*$ + MgO)–K_2O/Na_2O, (b) ($Fe_2O_3^*$ + MgO)–$Al_2O_3/(CaO + Na_2O)$, (c) ($Fe_2O_3^*$ + MgO)–Al_2O_3/SiO_2, and (d) ($Fe_2O_3^*$ + MgO)–TiO_2 (Bhatia, 1983) for the Lower Jurassic sandstones in the Onon fragment of the Aga Terrane. Fields that characterize sandstones from the following tectonic settings: A, oceanic island arcs; B, continental island arcs; C, active continental margins; D, passive continental margins.

the lower limiting depositional age of the protoliths of the schists of the Aga–Borshchovochnyi complex in the Nynken River basin, according to the results of U–Th–Pb (LA–ICP–MS) dating of detrital zircons, is 492 ± 6 Ma (Popeko et al., 2020), rocks of various ages are presently included in the Aga–Borshchovochnyi complex. It should be noted as well that the Early Mesozoic concordant age values were also obtained earlier for the youngest detrital zircon populations in the Paleozoic (?) metasedimentary rocks of the Tukuringra fragment of the Aga Terrane (Zaika et al., 2018) and the Dzhagdy Terrane (Sorokin et al., 2020) of the Mongol–Okhotsk Fold Belt. Consequently, the Mesozoic terrigenous deposits are most widespread in the Mongol–Okhotsk Fold Belt, Eastern Transbaikalia in particular.

Secondly, the U–Th–Pb dating of detrital zircons enables one not only to adjust the lower depositional age limit of the sedimentary strata but also to reconstruct the main detrital material source areas. According to the obtained data, the Paleozoic and Mesozoic detrital zircon grains characterized by the Neo- and

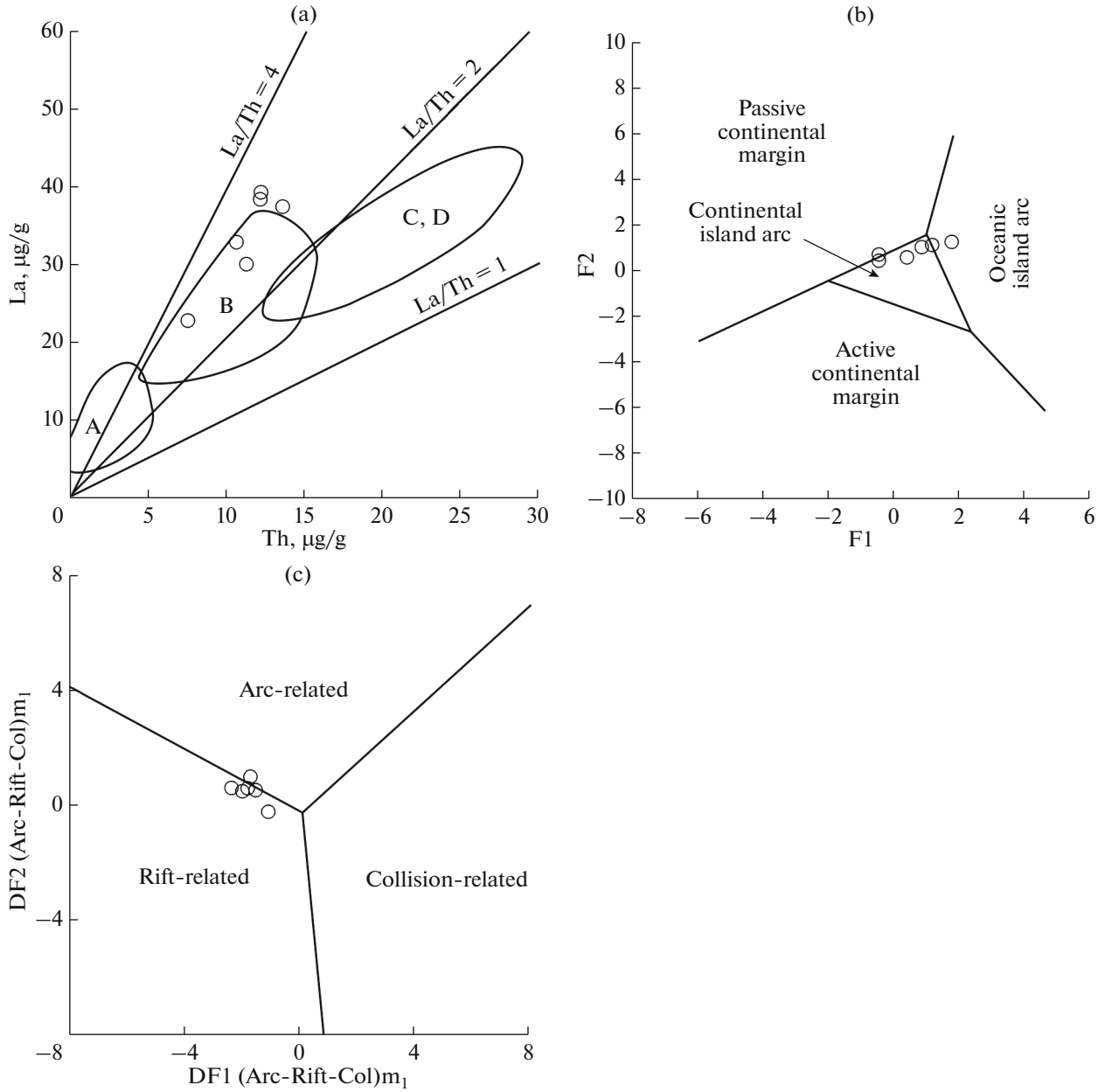

Fig. 9. Diagrams (a) Th–La (Bhatia and Crook, 1986); (b) F1–F2 (Bhatia, 1983), and (c) $DF1_{(Arc-Rift-Col)m1}$–$DF2_{(Arc-Rift-Col)m1}$ (Verma and Armstrong-Altrin, 2013) for the Lower Jurassic sandstones in the Onon fragment of the Aga Terrane. (a) Fields that characterize sandstones from the following tectonic settings: A, oceanic island arcs; B, continental island arcs; C, active continental margins; D, passive continental margins. (b) $F1 = 0.303 - 0.0447SiO_2 - 0.972TiO_2 + 0.008Al_2O_3 - 0.267 \times 0.74Fe_2O_3^* + 0.208 \times 0.23Fe_2O_3^* - 3.082MnO + 0.14MgO + 0.195CaO + 0.719Na_2O - 0.032K_2O + 7.51P_2O_5$; $F2 = 43.57 - 0.421SiO_2 + 1.988TiO_2 - 0.526Al_2O_3 - 0.551 \times 0.74Fe_2O_3^* - 1.61 \times 0.23Fe_2O_3^* + 2.72MnO + 0.881MgO - 0.907CaO - 0.177Na_2O - 1.84K_2O + 7.244P_2O_5$. (c) $DF1_{(Arc-Rift-Col)m1} = (-0.263\ln(TiO_2/SiO_2)_{adj}) + (0.604\ln(Al_2O_3/SiO_2)_{adj}) + (-1.725\ln(Fe_2O_3^*/SiO_2)_{adj}) + (0.660\ln(MnO/SiO_2)_{adj}) + (2.191\ln(MgO/SiO_2)_{adj}) + (0.144\ln(CaO/SiO_2)_{adj}) + (-1.304\ln(Na_2O/SiO_2)_{adj}) + (0.054\ln(K_2O/SiO_2)_{adj}) + (-0.330\ln(P_2O_5/SiO_2)_{adj}) + 1.588$; $DF2_{(Arc-Rift-Col)m1} = (-1.196\ \ln(TiO_2/SiO_2)_{adj}) + (1.064\ln(Al_2O_3/SiO_2)_{adj}) + (0.303\ln(Fe_2O_3^*/SiO_2)_{adj}) + (0.436\ln(MnO/SiO_2)_{adj}) + (0.838\ln(MgO/SiO_2)_{adj}) + (-0.407\ln(CaO/SiO_2)_{adj}) + (1.021\ln(Na_2O/SiO_2)_{adj}) + (-1.706\ \ln(K_2O/SiO_2)_{adj}) + (-0.126\ln(P_2O_5/SiO_2)_{adj}) - 1.068$.

Mesoproterozoic Hf model ages ($t_{Hf(C)}$ in the range of 0.7–1.3 Ga) are predominant in the sandstones studied. The igneous rock complexes of the Caledonian and Hercynian island arc systems of the ancient paleocean, which separated the Siberian Craton from the Amur Superterrane during the Paleozoic, could have been the main sources of the Paleozoic zircons (Gordienko, 2006; Gordienko et al., 2010, 2019). The most

probable sources of the youngest Mesozoic zircons are the rocks of the Early Mesozoic volcanoplutonic complex of the Aga Terrane (Ruzhentsev and Nekrasov, 2009; Shivokhin et al., 2010).

Obviously the sources of the insignificant Neoproterozoic detrital zircon population are the rocks of the Ikat–Bagdarin zone (Nekrasov et al., 2006, 2007) and the Kelyan and Kataev island arc systems (Gordienko, 2006). The oldest Paleoproterozoic zircon grains were most probably derived from the Paleoproterozoic granitoids (Donskaya, 2019; Donskaya et al., 2005; Sal'nikova et al., 2007; etc.) and gabbro-anorthosites (Buchko et al., 2008) at the southern surroundings of the Siberian Craton, which were involved in the sediment accumulation process.

Now let us turn to the geodynamic setting of sedimentation. Firstly, the chemical composition of the studied sandstones corresponds to greywacke; the clastic material in these rocks is poorly sorted; the clasts are angular and subrounded and include volcanic rock fragments. Secondly, the low degree of chemical "maturity" of the source rocks, their similarity in chemical composition to the rocks formed in active continental margin and island arc settings, and the presence of Early Jurassic detrital zircons in large amounts suggest sandstone accumulation during a period of high tectonic and igneous activity in the region. These data, coupled with the existing formation models of the terranes that make up the Mongol–Okhotsk Fold Belt (Arzhannikova et al., 2022; Gordienko, 2006; Gordienko et al., 2019; Parfenov et al., 2001; Ruzhentsev and Nekrasov, 2009; Shevchenko et al., 2014; etc.), suggest that the Lower Jurassic sandstones reflect the final phase of subduction in the structure of the Aga Terrane.

CONCLUSIONS

The main results of our studies are as follows:

(1) The sandstones of the Tutkhaltui Valley are characterized by closely similar variations of the chemical composition and correspond to the greywackes formed as a result of erosion of chemically "immature" predominantly felsic protoliths.

(2) The main sources of detrital material were the Mesozoic and Paleozoic igneous rocks with an insignificant contribution of the older Neo- and Paleoproterozoic igneous rocks.

(3) The age of the youngest population of detrital zircons from the sandstones of the Tutkhaltui Valley is 196 ± 8 Ma; consequently, their lower limiting depositional age corresponds to the Early Jurassic and, consequently, the sandstones studied reflect the Early Jurassic rather than Middle Paleozoic evolution stage of the Aga Terrane.

(4) The positions of data points of the studied sandstones on tectonic discrimination diagrams coupled with their mineralogical and petrographic features and the presence of a significant Early Jurassic detrital zircon population suggest their accumulation in a setting associated with subduction processes, which agrees with the existing geodynamic models of the evolution of the Mongol–Okhotsk Fold Belt.

ACKNOWLEDGMENTS

We are grateful to the laboratory staff at the Institute of Geology and Nature Management, Far Eastern Branch, Russian Academy of Sciences (E.N. Voropaeva, O.G. Medvedeva, V.I. Rozhdestvina, E.S. Sapozhnik, and E.V. Ushakova), and the Institute of Tectonics and Geophysics, Far Eastern Branch, Russian Academy of Sciences (V.E. Zazulina, E.M. Golubeva, and A.V. Shtareva), as well as the staff of the Arizona LaserChron Center, United States), for analytical studies.

CONFLICT OF INTEREST

The authors declare that they have no conflicts of interest.

Reviewers: S.I. Dril' and A.B. Kotov

REFERENCES

Amantov, V.A., Tectonics and formations of the Transbaikalia and Northern Mongolia, in *Tr. VSEGEI. T. 213* (Trans. Russ. Geol. Res. Inst. Vol. 213), Leningrad: Nedra, 1975 [in Russian].

Amelin, Y. and Davis, W.J., Geochemical test for branching decay of ^{176}Lu, *Geochim. Cosmochim. Acta*, 2005, vol. 69, pp. 465–473.

Arzhannikova, A.V., Demonterova, E.I., Jolivet, M., Arzhannikov, S.G., Mikheeva, E.A., Ivanov, A.V., Khubanov, V.B., and Pavlova, L.A., Late Mesozoic topographic evolution of western Transbaikalia: evidence for rapid geodynamic changes from the Mongol–Okhotsk collision to widespread rifting, *Geosci. Front.*, 2020, vol. 11, pp. 1695–1709.

Arzhannikova, A.V., Demonterova, E.I., Jolivet, M., Mikheeva, E.A., Ivanov, A.V., Arzhannikov, S.G., Khubanov, V.B., and Kamenetsky, V.S., Segmental closure of the Mongol-Okhotsk Ocean: insight from detrital geochronology in the East Transbaikalia Basin, *Geosci. Front.*, 2022, vol. 13, 101254.

Badarch, G., Cunningham, W.D., and Windley, B.F., A new terrane subdivision for Mongolia: Implications for the Phanerozoic crustal growth of Central Asia, *J. Asian Earth Sci.*, 2002, vol. 21, pp. 87–110.

Bhatia, M.R., Plate tectonics and geochemical composition of sandstones, *J. Geol.*, 1983, vol. 91, no. 6, pp. 611–627.

Bhatia, M.R. and Crook, K.A.W., Trace element characteristics of graywackes and tectonic setting discrimination of sedimentary basins, *Contrib. Mineral. Petrol.*, 1986, vol. 92, pp. 181–193.

Bogach, G.I., The petrology of tectonoblastites of the Aga–Borshchovochnyi complex, in *Geologiya i poleznye iskopaemye Chitinskoi oblasti* (Geology and Mineral Resources of the Chita Region), Asoskov, V.M., Ed., Chita: GGUP Chitageols'emka, 2000, pp. 172–178.

Bouvier, A., Vervoort, J.D., and Patchett, P.J., The Lu–Hf and Sm–Nd isotopic composition of CHUR: constraints from unequilibrated chondrites and implications for the

bulk composition of terrestrial planets, *Earth Planet. Sci. Lett.*, 2008, vol. 273, pp. 48–57.

Buchko, I.V., Sorokin, A.A., Sal'nikova, E.B., Kotov, A.B., Larin, A.M., Sorokin, A.P., Velikoslavinskii, S.D., and Yakovleva, S.Z., Age and tectonic setting of the Kengurak–Sergachi gabbro-anorthosite massif (the Selenga-Stanovoi superterrane, southern frame of the Siberian craton), *Stratigr. Geol. Correl.*, 2008, vol. 16, no. 4, pp. 349–359.

Bussien, D., Gombojav, N., Winkler, W., and Quadt, A.V., The Mongol–Okhotsk belt in Mongolia—An appraisal of the geodynamic development by the study of sandstone provenance and detrital zircons, *Tectonophysics*, 2011, vol. 510, pp. 132–150.

Condie, K.C., Chemical composition and evolution of the upper continental crust: Contrasting results from surface samples and shales, *Chem. Geol.*, 1993, vol. 104, pp. 1–37.

Cullers, R.L., Implications of elemental concentrations for provenance, redox conditions, and metamorphic studies of shales and limestones near Pueblo, CO, USA, *Chem. Geol.*, 2002, vol. 191, pp. 305–327.

Demonterova, E.I., Ivanov, A.V., Mikheeva, E.M., Arzhannikova, A.V., Frolov, A.O., Arzhannikov, S.G., Bryanskiy, N.V., and Pavlova, L.A., Early to Middle Jurassic history of the southern Siberian continent (Transbaikalia) recorded in sediments of the Siberian Craton: Sm–Nd and U–Pb provenance study, *Bull. Soc. Géol. Fr.*, 2017, vol. 188. 8.

Didenko, A.N., Kaplun, V.B., Malyshev, Yu.F., and Shevchenko, B.F., The lithospheric structure and Mesozoic geodynamics eastern Central Asian fold belt, *Russ. Geol. Geophys.*, 2010, vol. 51, no. 5, pp. 629–647.

Donskaya, T.V., The Early Proterozoic Granitoid Magmatism of the Siberian Craton, *Doctoral (Geol.-Mineral.) Dissertation*, Irkutsk: Inst. Zemn. Kory Sib. Otd. Ross. Akad. Nauk, 2019.

Donskaya, T.V., Gladkochub, D.P., Kovach, V.P., and Mazukabzov, A.M., Petrogenesis of Early Proterozoic postcollisional granitoids in the southern Siberian Craton, *Petrology*, 2005, vol. 13, no. 3, pp. 229–252.

Floyd, P.A. and Leveridge, B.E., Tectonic environment of the Devonian Gramscatho basin, south Cornwall: Framework mode and geochemical evidence from turbiditic sandstones, *J. Geol. Soc. London*, 1987, vol. 144, no. 4, pp. 531–542.

Geodinamika, magmatizm i metallogeniya vostoka Rossii (Geodynamics, Magmatism, and Metallogeny of the Russian East), Khanchuk, A.I., Ed., Vladivostok: Dalnauka, 2006, Book 1 (in Russian),

Gordienko, I.V., Geodynamic evolution of Late Baikalides and Paleozoides in the folded periphery of the Siberian Craton, *Russ. Geol. Geophys.*, 2006, vol. 47, no. 1, pp. 51–67.

Gordienko, I.V., Bulgatov, A.N., Ruzhentsev, S.V., Minina, O.R., Klimuk, V.S., Vetluzhskikh, L.I., Nekrasov, G.E., Lastochkin, N.I., Sitnikova, V.S., Metelkin, D.V., Goneger, T.A., and Lepekhina, E.N., The Late Riphean–Paleozoic history of the Uda–Vitim island arc system in the Transbaikalian sector of the Paleoasian Ocean, *Russ. Geol. Geophys.*, 2010, vol. 51, no. 5, pp. 461–481.

Gordienko, I.V., Metelkin, D.V., and Vetluzhskikh, L.I., The structure of the Mongol–Okhotsk Fold Belt and the problem of recognition of the Amur microcontinent, *Russ. Geol. Geophys.*, 2019, vol. 60, no. 3, pp. 267–286.

Griffin, W.L., Belousova, E.A., Shee, S.R., Pearson, N.J., and O'Reilly, S.Y., Archean crustal evolution in the northern Yilgarn Craton: U–Pb and Hf-isotope evidence from detrital zircons, *Precambrian Res.*, 2004, vol. 131, pp. 231–282.

Hara, H., Kurihara, T., Tsukada, K., Kon, Y., Uchino, T., Suzuki, T., Takeuchi, M., Nakane, Y., Nuramkhaan, M., and Chuluun, M., Provenance and origins of a Late Paleozoic accretionary complex within the Khangai–Khentei belt in the Central Asian Orogenic Belt, central Mongolia, *J. Asian Earth Sci.*, 2013, vol. 75, pp. 141–157.

Harnois, L., The CIW index: A new chemical index of weathering, *Sediment. Geol.*, 1988, vol. 55, nos. 3–4, pp. 319–322.

Herron, M.M., Geochemical classification of terrigenous sands and shales from core or log data, *J. Sediment. Petrol.*, 1988, vol. 58, pp. 820–829.

Jayawardena, U.S. and Izawa, E., A new chemical index of weathering for metamorphic silicate rocks in tropical regions: A study from Sri Lanka, *Eng. Geol.*, 1994, vol. 36, pp. 303–310.

Kelty, T.K., Yin, A., Dash, B., Gehrels, G.E., and Ribeiro, A.E., Detrital-zircon geochronology of Paleozoic sedimentary rocks in the Hangay–Hentey basin, north-central Mongolia: Implications for the tectonic evolution of the Mongol–Okhotsk Ocean in central Asia, *Tectonophysics*, 2008, vol. 451, pp. 290–311.

Ludwig, K.R., Isoplot 3.6, *Berkeley Geochronol. Center Spec. Publ.*, 2008, no. 4.

Lykhin, D.A., Presnyakov, S.L., Nekrasov, G.E., Ruzhentsev, S.V., Golionko, B.G., and Balashova, Yu.S., Geodynamic problems of the junction between the Agin and Argun zones of Transbaikalia: Evidence from U–Pb SHRIMP dating of rocks of the Tsugol gabbro-plagiogranite massif, *Dokl. Earth Sci.*, 2007, vol. 417, no. 2, pp. 1407–1411.

McDonough, W.F. and Sun, S.-S., The composition of the Earth, *Chem. Geol.*, 1995, vol. 120, pp. 223–253.

Metelkin, D.V., Vernikovsky, V.A., Kazannsky, A.Y., and Wingate, M.T.D., Late Mesozoic tectonics of Central Asia based on paleomagnetic evidence, *Gondwana Res.*, 2010, vol. 18, pp. 400–419.

Nekrasov, G.E., Ruzhentsev, S.V., Presnyakov, S.L., Rodionov, N.V., Lykhin, D.A., and Golionko, B.G., U–Pb SHRIMP zircon dating of plutonic and metamorphic rocks of the Ikat–Bagdarin and Aga zones (Transbaikalia), in *Mater. nauchn. soveshch. "Geodinamicheskaya evolyutsiya litosfery Tsentral'no-Aziatskogo podvizhnogo poyasa (ot okeana k kontinentu)"* (Proc. Sci. Conf. "Geodynamic Evolution of Lithosphere of the Central Asian Fold Belt (From Ocean to Continent)"), Sklyarov, E.V., Ed., Irkutsk: Inst. Zemn. Kory Sib. Otd. Ross.Akad. Nauk, 2006, vol. 2, pp. 58–60.

Nekrasov, G.E., Rodionov, N.V., Berezhnaya, N.G., Sergeev, S.A., Ruzhentsev, S.V., Minina, O.R., and Golionko, B.G., U–Pb age of zircons from plagiogranite veins in migmatized amphibolites of the Shaman Range (Ikat–Bagdarin Zone, Vitim Highland, Transbaikal Region), *Dokl. Earth Sci.*, 2007, vol. 413, pp. 160–163.

Nokleberg, W.J., Bundtzen, T.K., Eremin, R.A., Ratkin, V.V., Dawson, K.M., Shpikerman, V.I., Goryachev, N.A., Byalobzhesky, S.G., Frolov, Y.F., Khanchuk, A.I., Koch, R.D., Monger, J.W.H., Pozdeev, A.I., Rozenblum, I.S., Rodionov, S.M., Parfenov, L.M., Scotese, C.R., and Sidorov, A.A., Metallogenesis and tectonics of the Russian Far East, Alaska, and the Canadian Cordillera, *U.S. Geol. Surv. Prof. Pap.*, 2005, no. 1697.

Parfenov, L.M., Popeko, L.I., and Tomurtogoo, O., Problems of tectonics of the Mongol-Okhotsk orogenic belt, *Geol. Pac. Ocean*, 2001, vol. 16, pp. 797–830.

Parfenov, L.M., Berzin, N.A., Khanchuk, A.I., Bodarch, G., Belichenko, V.G., Bulgatov, A.N., Dril, S.I., Kirillova, G.L., Kuzmin, M.I., Nokleberg, W.J., Prokopyev, A.V., Timofeev, V.F., Tomurtogoo, O., and Yang, H., A model for the formation of orogenic belts of Central and Northeast Asia, *Tikhookean. Geol.*, 2003, vol. 22, no. 6, pp. 7–41.

Pettijohn, F. J.; Potter, P. E.; and Siever, R., *Sand and Sandstone*, Berlin, 1972.

Popeko, L.I., Smirnova, Y.N., Zaika, V.A., Sorokin, A.A., and Dril, S.I., Provenance and tectonic implications of sedimentary rocks of the Paleozoic Chiron Basin, Eastern Transbaikalia, Russia, based on whole-rock geochemistry and detrital zircon U–Pb age and Hf isotopic data, *Minerals*, 2020, vol. 10.
https://doi.org/10.3390/min10030279

Rutshtein, I.G., The problems of geology and regional metallogeny of southeastern Transbaikalia, in *Geologiya i poleznye iskopaemye Chitinskoi oblasti* (Geology and Mineral Recourses of the Chita Region), Asoskov, V.M., Ed., Chita, GGUP Chitageols'emka, 2000, pp. 9–23.

Rutshtein, I.G., Bogach, G.I., Enikeev, F.I., and Vavilov, D.E., *Geologicheskaya karta Rossiiskoi Federatsii masshtaba 1 : 200000. Vostochno-Zabaikal'skaya seriya. List M-50-II* (The 1 : 200 000 Geological Map of the Russian Federation. East Transbaikalian Ser. Sheet M-50-II), St. Petersburg: Vseross. Nauchno-Issled. Geol. Inst., 2019.

Ruzhentsev, S.V. and Nekrasov, G.E., Tectonics of the Aga Zone, Mongolia-Okhotsk belt, *Geotectonics*, 2009, vol. 43, no. 1, pp. 34–50.

Sal'nikova, E.B., Kotov, A.B., Levitskii, V.I., Reznitskii, L.Z., Mel'nikov, A.I., Kozakov, I.K., Kovach, V.P., Barash, I.G., and Yakovleva, S.Z., Age constraints of high-temperature metamorphic events in crystalline complexes of the Irkut block, the Sharyzhalgai ledge of the Siberian platform basement: Results of the U-Pb single zircon dating, *Stratigr. Geol. Correl.*, 2007, vol. 15, no. 4, pp. 343–358.

Scherer, E., Münker, C., and Mezger, K., Calibration of the lutetium-hafnium clock, *Science*, 2001, vol. 293, pp. 683–687.

Shevchenko, B.F., Popeko, L.I., and Didenko, A.N., Tectonics and evolution of the lithosphere of the eastern fragment of the Mongol–Okhotsk orogenic belt, *Geodynam. Tektonophys.*, 2014, vol. 5, no. 3, pp. 667–682.

Shivokhin, E.A., Ozerskii, A.F., Kurilenko, A.V., Raitina, N.I., and Karasev, V.V., *Gosudarstvennaya geologicheskaya karta Rossiiskoi Federatsii masshtaba 1 : 1000000 (tret'e pokolenie). Aldano-Zabaikal'skaya seriya. List M-50 (Borzya)* (The 1 : 1 000000 State Geological Map of the Russian Federation (3rd ed.). Aldan–Transbaikal. Ser. Sheet M-50 (Borzya)), Starchenko, V.V., Ed., St. Petersburg: Vseross. Nauchno-Issled. Geol. Inst., 2010.

Söderlund, U., Patchett, P.J., Vervoort, J.D., and Isachsen, C.E., The ^{176}Lu decay constant determined by Lu–Hf and U–Pb isotope systematics of Precambrian mafic intrusions, *Earth Planet. Sci. Lett.*, 2004, vol. 219, pp. 311–324.

Sorokin, A.A., Kolesnikov, A.A., Kotov, A.B., Sorokin, A.P., and Kovach, V.P., Sources of detrital zircons from terrigenous deposits in the Yankan terrane of the Mongolian-Okhotsk mobile belt, *Dokl. Earth Sci.*, 2015, vol. 462, no. 5, pp. 621–625.

Sorokin, A.A., Zaika, V.A., Kovach, V.P., Kotov, A.B., Xu, W., and Yang, H., Timing of closure of the eastern Mongol-Okhotsk Ocean: constraints from U–Pb and Hf isotopic data of detrital zircons from metasediments along the Dzhagdy Transect, *Gondwana Res.*, 2020, vol. 81, pp. 58–78.

Taylor, S.R. and McLennan, S.M., *The Continental Crust: Its Composition and Evolution*, Blackwell, Oxford, 1985.

Tomurtogoo, O., Windley, B.F., Kröner, A., Badarch, G., and Liu, D.Y., Zircon age and occurrence of the Adaatsag ophiolite and Muron shear zone, central Mongolia: constraints on the evolution of the Mongol–Okhotsk ocean, suture and orogen, *J. Geol. Soc.*, 2005, vol. 162, pp. 125–134.

Tulokhonov, M.I., *Geologicheskaya karta SSSR masshtaba 1 : 200000. Vostochno-Zabaikal'skaya seriya. List M-50-II* (The 1 : 200000 Geological Map of the USSR. East Transbaikal. Ser. Sheet M-50-II), Muzylev, S.A., Ed., Moscow: Gosgeoltekhizdat, 1962 [in Russian].

Verma, S.P. and Armstrong-Altrin, J.S., New multi-dimensional diagrams for tectonic discrimination of siliciclastic sediments and their application to Precambrian basins, *Chem. Geol.*, 2013, vol. 355, pp. 117–133.

Vervoort, J.D. and Patchett, P.J., Behavior of hafnium and neodymium isotopes in the crust: constraints from Precambrian crustally derived granites, *Geochim. Cosmochim. Acta*, 1996, vol. 60, pp. 3717–3723.

Wang, W., Tang, J., Xu, W.L., and Wang, F., Geochronology and geochemistry of Early Jurassic volcanic rocks in the Erguna Massif, northeast China: Petrogenesis and implications for the tectonic evolution of the Mongol–Okhotsk suture belt, *Lithos*, 2015, vol. 218–219, pp. 73–86.

Wronkiewicz, D.J. and Condie, K.C., Geochemistry of Archean shales from the Witwatersrand Supergroup, South Africa: Source-area weathering and provenance, *Geochim. Cosmochim. Acta*, 1987, vol. 51, no. 9, pp. 2401–2416.

Yang, Y.T., Guo, Z.-X., Song, C.-C., Li, X.-B., and He, S., A short-lived but significant Mongol-Okhotsk collisional orogeny in latest Jurassic–earliest Cretaceous, *Gondwana Res.*, 2015, vol. 28, pp. 1096–1116.

Zaika, V.A. and Sorokin, A.A., Two types of accretionary complexes in the eastern Mongol–Okhotsk Belt: Constraints from U–Pb and Hf isotopic data of detrital zircons from metasedimentary rocks of the Selemdzha and Tokur terranes, *J. Asian Earth Sci.*, 2020a, vol. 201, 104508.

Zaika, V.A. and Sorokin, A.A., Ages and sources of sedimentary rocks of the Lan Terrane in the Mongol-Okhotsk Fold Belt: Results of Zircon U–Pb and Lu–Hf isotope studies, *Russ. J. Pac. Geol.*, 2020b, vol. 14, pp. 193–205.

Zaika, V.A., Sorokin, A.A., Xu, B., Kotov, A.B., and Kovach, V.P., Geochemical features and sources of metasedimentary rocks of the western part of the Tukuringra Terrane of the Mongol–Okhotsk Fold Belt, *Stratigr. Geol. Correl.*, 2018, vol. 26, no. 2, pp. 157–178.

Zhao, X., Coe, R.S., Zhou, Y., Wu, H., and Wang, J., New paleomagnetic results from northern China: collision and suturing with Siberia and Kazakhstan, *Tectonophysics*, 1990, vol. 181, pp. 43–81.

Zonenshain, L.P., Kuz'min, M.I., and Natapov, L.M., *Tektonika litosfernykh plit territorii SSSR* (Tectonics of the Lithospheric Plates in the USSR), Moscow: Nedra, 1990, Book 1.

Zorin, Yu.A., Geodynamics of the western part of the Mongolia-Okhotsk collisional belt, Trans-Baikal region (Russia) and Mongolia, *Tectonophysics*, 1999, vol. 306, pp. 33–56.

Translated by E. Murashova